JURNAL SEGARA
http://ejournal-balitbang.kkp.go.id/index.php/segara

ISSN : 1907-0659
e-ISSN : 2461-1166
Nomor Akreditasi: 766/AU3/P2MI-LIPI/10/2016

MODELING TIDAL CURRENT OF BANTEN BAY DURING TRANSITIONAL MONSOONS

PEMODELAN ARUS PASANG SURUT TELUK BANTEN PADA MUSIM PERALIHAN

Ahmad Bayhaqi[1)], Ulung J. Wisha[2)] & Dewi Surinati[1)]

[1)]Physical Oceanography and Climate Laboratory, Research Center for Oceanography, Indonesian Institute of Sciences, Jl. Pasir Putih 1, North Jakarta, 14430, Indonesia
[2)]Research Institute for Coastal Resources and Vulnerability, Ministry of Marine Affairs Jl. Raya Padang-Painan KM 16, Padang, 25245, Indonesia

Received: 17 May 2016; Revised: 19 May 2016; Accepted: 31 August 2016

ABSTRCT

Hydrodynamic condition of Java sea as a part of Indian-Pacific throughflow system influenced by monsoon will affect the condition of Banten Bay such as tidal current. Bordered by Java Sea makes Banten Bay preoccupied with fisheries and shipping activities, so the information regarding current pattern that is tidal current is very necessary. This study aims to simulate the tidal current pattern using flow model fm as a numerical approach. Two-dimensional hydrodynamic model was employed to perform the simulation of tidal current. Model was validated by using current and tidal observation data which was taken in September 2015 and April 2016. Results show that the current moves southwestern toward the land during high neap and high spring tidal conditions ranged 0 - 0.142 m/s at the first transitional monsoon and 0 - 0.153 m/s at the second transitional monsoon respectively. During low spring tidal condition for both transitional monsoons, the current flowed northwestward on west side and northeastward on east side within the bay ranged 0 - 0.137 m/s and 0 - 0.127 m/s respectively. The hydrodynamic conditions of Banten Bay are slightly different between 2 transitional seasons, especially for the current speed and direction. Those conditions induce a different transport mechanism, resulting in unstable accretion and abrasion along Banten Bay coast.

Keywords: Tidal current modeling, Banten Bay, transitional monsoons.

Corresponding author:
Jl. Pasir Putih I Ancol Timur, Jakarta Utara 14430. Email: ulungjantama@gmail.com

DOI: http://dx.doi.org/10.15578/segara.v14i2.6452

INTRODUCTION

Banten Bay is located in the northern coast and northwest tip of Java Island. The water is directly adjacent to the Java Sea. Globally, Java Sea is part of Pacific-Indian Ocean flow system through Indonesian Seas known as Indonesian Throughflow (ITF). The Indonesian seas become a link between the tropical Pacific and the Indian Ocean in which the main throughflow pathway sources from Makassar Strait (Gordon *et al*., 2010). It is obvious why Makassar Strait is the main gate for ITF entering the Indonesian Seas (Lukas *et al*., 1996). However, for the western region, Pacific water mass flows into the Indonesian seas through the South China Sea moving toward the Java Sea through Karimata Strait (Fang *et al*., 2010) and leaks to Indian Ocean through Sunda Strait.

In general, Java Sea is predominantly influenced by the monsoon condition. ITF becomes stronger during East monsoon and weaker during West monsoon. Throughflow and monsoons have a big role evoking variability of water mass transport in the Java Sea (Siregar *et al*., 2017). The wind predomination on each monsoon triggers fluctuation of significant wave height in the straits of Java (Wicaksana *et al*., 2015). On the boreal winter monsoon (November-March), the Java Sea becomes a container of low salinity water masses flow from the South China Sea moving strongly toward the east. It affects the transport of ITF from Makassar Strait which will move to the Indian Ocean (Gordon *et al*., 2003; Gordon *et al*., 2012; Qu *et al*.,2006; Fang *et al*., 2009; Tozuka *et al*., 2009; Susanto *et al*., 2012; Susanto *et al*., 2013) through the main exit gates, such as Lombok Strait, Ombai Strait and Timor Gap (Susanto *et al*., 2016). The Sunda Strait, the nearest strait from Banten Bay in the west side, separates the Sumatera and Java Islands has a role in the circulation of Pacific-Indian water masses becoming the exit gap for Java Sea water with higher temperature and low density toward the Indian Ocean in May-September (Susanto *et al*., 2016).

Based on the geographical perspective, Banten Bay is a significance region to study about water hydrodynamics such as tidal current. Tidal is elevation fluctuation in the ocean which is generated by gravitational forces of the moon and the sun (Douglas, 2001; Kvale, 2006). It triggers the ocean current (tidal current) (Stewart, 2006). The circulation pattern occurred in the Java Sea during northwest and southeast monsoon is expected to give an influence on the water condition of Banten Bay.

As a semi-enclosed water area, hydrodynamic within Banten Bay tends to be weaker. In the bay mouth, there are several islands (Panjang Island, Fie Island, and Tiga Island) contributing the water flow deformation while passing those islands. These three islands may have a significance impact on tidal current movement within the bay (Hoekstra *et al*., 2002). The current profile within the bay is unstable, the ocean current from Sunda Strait takes place several times, resulting in dramatic alteration of current speed (Wisha *et al*., 2015). While, near the coast, there are some small islands, they are Tarakan Island in the west part within the bay, Kubur and Lima Islands in the middle near the bay mouth, Satu and Dua Islands in the southeast coast. Those small islands should have a role influencing longshore current profile within the bay. In addition, some small islands run into erosion and sedimentation impacted by sand mining in the northern of the bay triggering the unstable transport sediment in and out of the bay (Rahmawan *et al*., 2017).

One of the worst problems occurred in Banten Bay is sand mining activity. It started from 2003 and stopped for a while in 2013, resulting in altered morphology around Lontar Village coast (Rahmawan *et al*., 2017). It also influences Ciujung delta formation. It proves that the accretion has been occurred, impacting the delta appearance. The worse impact is coastal stability disruption. Several area experiences erosion and the other area experiences sedimentation. Hydrodynamic pattern has a big role controlling turbulence and mixing which the sediment transport takes place. It has different characteristics and impacts in every single monsoon due to the vary wind direction and stress.

To reveal the condition between two seasons, the study in the transition monsoon is very essential to do as well. In addition, Banten Bay is classified as busy region with human, fisheries and shipping activities. The information of current pattern including tidal current is necessary to support those activities. One of the ways to study regarding tidal current pattern is model approach using numerical simulation. This way can give a bigger depiction when the location can be fully covered by observation. The previous study (Wisha *et al*., 2015) illustrated the simulation of tidal current in Banten Bay. However, it was simulated only during the second transitional monsoon (September-October) in 2014. So, this study aims to examine the tidal current condition of 2 cycles transitional monsoon (2^{nd} transitional monsoon is represented by September 2015 simulation and 1st transitional monsoon is represented by April 2016 simulation).

METHODOLOGY

Observation was conducted in September 2015 (Second Transitional Monsoon) and April 2016 (First Transitional Monsoon). The method used to collect current data was mooring installation by using Acoustic Doppler Current Profiler (ADCP) Nortek and Recording

Current Meter (RCM) Aanderaa. Due to the technical problem, the tidal data was only taken on September 2015, so tidal prediction from Tide Model Driver (TMD) (King *et al*., 2011) was used to validate the April 2016 simulation. Bathymetry from Hydrography and Oceanography Center-Indonesian Navy (PUSHIDROSAL) sheet number 78, 15th edition December 2006, NOAA coastline data from A Global Self-Continent, Hierarchical, High-Resolution Geography (GSHHG) database (Wessel & Smith, 1996) and Global Tide Prediction data (Park *et al*., 2014) were applied as a data input in the model. The result of the model was depicted as a tidal current pattern for four extreme tidal conditions. These results were validated by observation data, employing Root Mean Squared Error (RMSE) formula (Spaulding & Mendelsohn, 1999) as follow:

$$\sqrt{\frac{1}{n}\sum_{i=1}^{n}(y-yi)^2} \quad \text{..... 1)}$$

where:
n = The number of total data
y = model result data
yi = observation data

Hydrodynamic Model Equation

The model used to perform the simulation of tidal current was flow model flexible mesh (fm) provided by MIKE Zero, 2007, SP2, two-dimensional hydrodynamic model. According to Mahardika *et al*. (2015), flow model fm can represent the real condition which is more accurate than the other method such as ADCIRC. The flow model consists of continuity and momentum equation (Zhao *et al*., 1994).

The continuity equation is written as:

$$\frac{\partial u}{\partial x}+\frac{\partial v}{\partial y}+\frac{\partial w}{\partial z}=S \quad \text{..... 2)}$$

The momentum equation for the Cartesian coordinate, respectively:

$$\frac{\partial u}{\partial t}+\frac{\partial u^2}{\partial x}+\frac{\partial vu}{\partial y}+\frac{\partial wu}{\partial z}=fv-g\frac{\partial \eta}{\partial x}-\frac{1}{\rho o}\frac{\partial Pa}{\partial x}-\frac{g}{\rho o}\int_z^{\eta}\frac{\partial \rho}{\partial x}dz+Fu+\frac{\partial}{\partial z}\left(vt\frac{\partial u}{\partial z}\right)+usS \quad \text{.. 3)}$$

$$\frac{\partial v}{\partial t}+\frac{\partial v^2}{\partial y}+\frac{\partial uv}{\partial x}+\frac{\partial wv}{\partial z}=-fu-g\frac{\partial \eta}{\partial y}-\frac{1}{\rho o}\frac{\partial Pa}{\partial y}-\frac{g}{\rho o}\int_z^{\eta}\frac{\partial \rho}{\partial y}dz+Fv+\frac{\partial}{\partial z}\left(vt\frac{\partial v}{\partial z}\right)+vsS \quad \text{.. 4)}$$

Where
t : time
x, y, z : cartesian coordinate
η : surface elevation
d : still water depth
u, v, w : velocity components in the x, y, and z direction
f : 2Ω sin ϕ (Coriolis parameter) where Ω is angular rate and ϕ is geographical latitude
g : gravitational acceleration
ρ : density
vt : vertical turbulent or eddy viscosity
Pa : atmospheric pressure
ρo : reference density

Research observation point

Field measurement points of current and tide data were located in the eastern Panjang Island (Figure 1), conducted twice to represent 2 phases of the transitional season. Mooring a (current meter) was deployed for 2 days measurement on April 2016 at 10-meters depth recording the current data only, while, the mooring b (ADCP) was deployed during September 2015 at 8-meters depth measuring the tidal and current data as well. The obtained data was then sorted by using Surge software to delete the bias data. Current data is provided in the form of layer data, we only used the uppermost layer near the surface adjusted to the model simulated. So that, they can be compared to evaluate the model built.

Model Set up

The simulation applied for transitional monsoons was adjusted with observation data. Flow model fm was built by the development of 2-dimensional flow equation spatially discretized and showed by cell-centered finite volume method (Zhao *et al*., 1994). This model was supported by a flexible mesh and tidal prediction, bordered by five boundary conditions for 1st Transitional simulation and three boundaries for 2nd Traditional simulation. Tide forecasting was employed as the model input, it is obtained by executing Ergtide software (Masoud *et al*., 2012). The model set-up for the 1st transitional simulation is shown in table 1 and for the 2nd transitional simulation is shown in Table 2 respectively.

The model simulated twice, appropriate with the field measurement time. Tidal currents simulation was simulated for 15 days, but the data will be displayed for four extreme tidal conditions. It represents the tidal current pattern during two transitional seasons (Carter & Merrifield, 2007). It displayed spatially in the form of hydrodynamical map. Second Transitional (September-October) hydrodynamic simulation in 2014 was studied by Wisha *et al*. (2015). We applied a modification on the year of simulation (2nd transitional season in 2015) which was in accordance with the period of tide

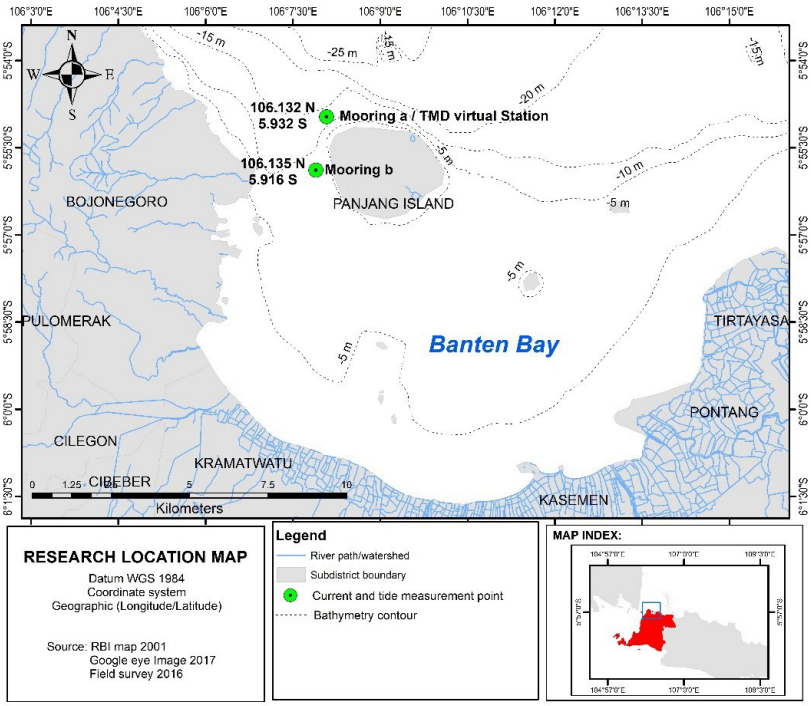

Figure 1. Research Location. Mooring a: Using RCM Aanderaa (1st Transitional Monsoon), this point was also employed to become the TMD virtual station. Mooring b: Using ADCP Nortek (2nd Transitional Monsoon).

forecasting data used as boundary condition. We also updated the coastline digitation used as a land boundary, besides, this brand-new model uses a different time step interval and total number of time step. Even though the bathymetry data are the same with the previous.

RESULTS AND DISCUSSION

Model Validation

The model was validated by comparing field measurement data and model result (Lazure *et al*., 2009; Wisha *et al*., 2017). In this study, sea level and

Table 1. Field observation results

Parameter	Implemented in the simulation
Time of simulation	Number of time step = 384 Time step interval = 3,600 sec Simulation start date = 14/04/2016 12.00 AM Simulation end date = 30/04/2016 12.00 AM
Mesh boundary	Bathymetry =PUSHIDROSAL Bathymetry map digitation
Flood and dry	Drying depth = 0.005 m Flooding depth = 0.05 m Wetting depth = 0.1 m
Wind forcing	Format = Varying in time, constant in domain Neutral pressure 103 hPa Soft start interval = 0 sec
Boundary condition	Type = Specified level Format = Varying in time, constant along boundary Time Series = Tide forecasting with coordinates below: 1. Longitude: 106.25058, Latitude: -5.9298 2. Longitude: 106.22785, Latitude: -5.9053 3. Longitude: 106.18982, Latitude: -5.8858 4. Longitude: 106.14632, Latitude: -5.8768 5. Longitude: 106.10313, Latitude: -5.8830

Table 2. Simulation Set up (2nd Transitional season)

Parameter	Implemented in the simulation
Time of simulation	Number of time step = 384 Time step interval = 3,600 sec Simulation start date = 01/09/2015 13.45 AM Simulation end date = 01/10/2015 12.45 AM
Mesh boundary	Bathymetry =PUSHIDROSAL + LPI Bathymetry map digitation
Flood and dry	Drying depth = 0.005 m Flooding depth = 0.05 m Wetting depth = 0.1 m
Wind forcing	Format = Varying in time, constant in domain Neutral pressure 103 hPa Soft start interval = 0 sec
Boundary condition	Type = Specified level Format = Varying in time, constant along boundary Time Series = Tide forecasting with coordinates below: 1. Longitude: 106.0410, Latitude: -5.8406 2. Longitude: 106.1828, Latitude: -5.7656 3. Longitude: 106.3227, Latitude: -5.8343

velocity component (U and V) are the parameter used to verify the model both for first and second transitional monsoon simulation. Overall, the comparison between model (blue line) and observation data (orange line) of surface elevation (Figure 2) shows the similarity in term of tidal phases. The RMSE value for both respectively is 5.9% and 11.89%. Based on the measurement, the tide type of Banten Bay is mixed tide prevailing diurnal, it was also explained by Wisha *et al*. (2015). According to Hoekstra *et al*. (2002) defined that the tidal regime was found to be mixed, predominantly diurnal, with a varying tidal range between 20-90 cm.

The 2nd transitional verification (Figure 2b) shows the unstable and volatile tidal phases during last neap tidal condition (red circle) and first neap tidal condition (blue circle). These disturbances are possibly triggered by the wind wave generation. Tidal changes followed by the low period of wave generation contribute to the formed elevation (Garrett & Kunze, 2007), resulting a rapid accretion along the shore edge.

Velocity component verification (Figure 3), shows that model result and observation have the same pattern but different in magnitude. The RMSE value for the zonal component in the first transitional monsoon

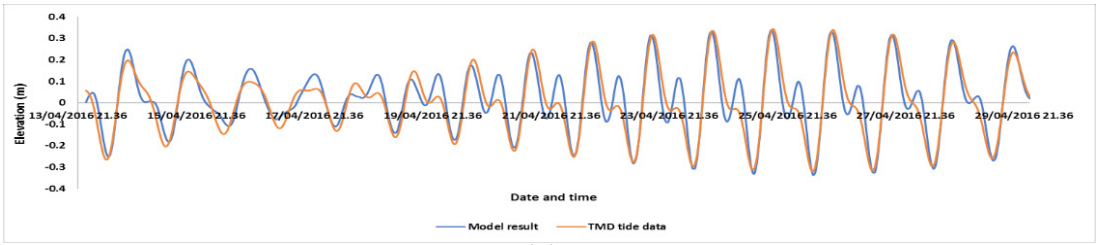

(a)

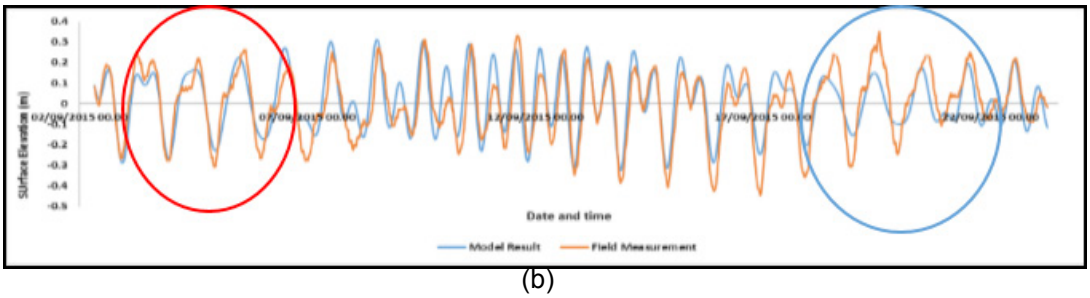

(b)

Figure 2. Surface elevation validation; a. Comparison between model and TMD-Observation Data, b. Comparison between model and ADCP data retrieval. Blue and red circles show the bias of surface elevation data during field measurement. It was found during two neap tidal conditions.

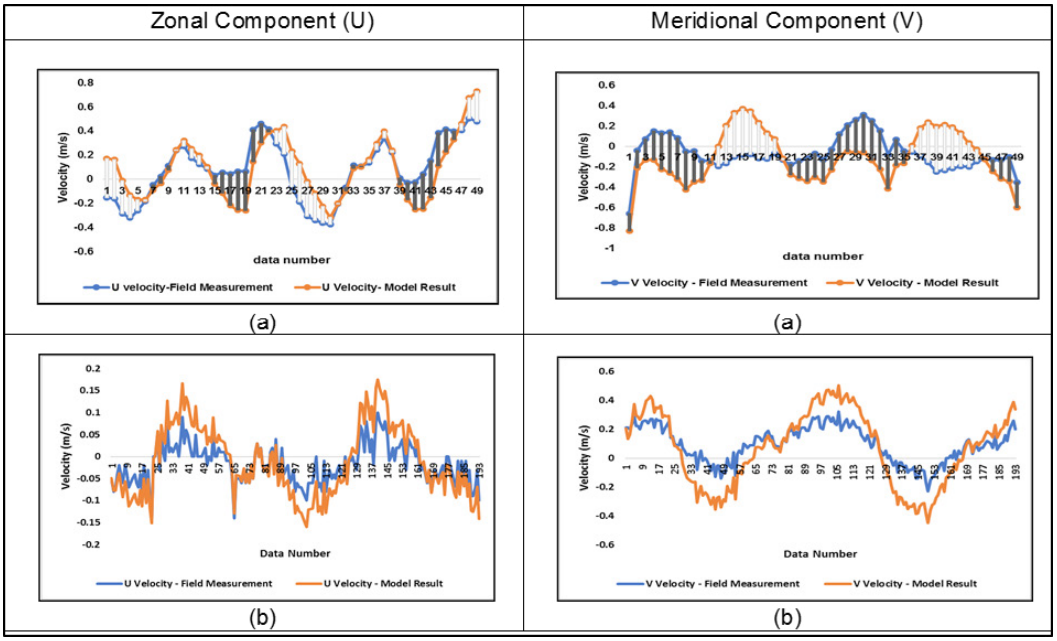

Figure 3. Velocity Component Comparison between Model Result and Observation on First Transitional (a) and Second Transitional Monsoon (b).

and the second are respectively 17.95% and 7.64%, while for the meridional components are 19.6% and 8.24%. For the first transitional simulation, RMSE value is greater than the second one because the data was taken in the fixed depth (10 meters beneath the surface). It is not really well representing the surface condition, in fact, the model is simulated the current pattern in the surface. While, for the second transitional monsoon, the data were taken at each level of depth, so that, the surface data can be well covered. However, the error value can be accepted if it does not exceed 40% (Holt *et al*., 2005), so we assume that this model is proper to figure out the field condition.

Figure 4 shows the current component velocity comparison between model result and field measurement in the form of vector magnitude and direction, at the 1st transitional season, the current velocity ranged from -0.4 to 0.49 m/s and from-0.21 to 0.23 m/s for field measurement and model result respectively, the direction differentiation is almost 3 degrees predominated toward West-Northwest and East-Southeast. Whilst, at the 2nd transitional season, the current velocity ranged from -0.13 to 0.2 m/s and from -0.18 to 0.28 m/s for field measurement and model result respectively, the direction is predominated toward North-Northwest and South-southeast with 5 degrees direction differentiation.

Ellipsoid velocity component analysis also shows that the tidal current is rotary. It flows continuously with the direction alteration amount 360 degree during the tidal period. According to Poulain (2013) the rotation of tidal current is caused by the earth's rotation even though it is depended on local condition. It moves clockwise in the northern hemisphere and counterclockwise in the southern hemisphere. Rotary current can be depicted as in Figure 4, it forms a series of arrows representing the direction and the speed of the current at each hour. Offshore rotary currents which are purely diurnal repeat the elliptical pattern each tidal condition of 12 hours and 25 minutes (Boon, 2013). In the both diurnal region, there is an obvious relationship between times of current and times of high and low water in the locality (Antony & Unnikrishnan, 2013).

Tidal Current Simulation

Tidal current pattern in Banten Bay water at the first transitional monsoon (Figure 5) moves southwestward. The velocity ranged from 0-0.142 m/s and 0-0.153 m/s respectively during high neap and high spring tidal condition. While, the current moves Northeastward at the neap low tidal condition, the speed ranged from 0-0.042 m/s. The current moves northeastward on the east side within the bay and northwestward on the west side within the bay during the spring low tidal condition, the speed ranged 0-0.137 m/s. During the second transitional monsoon (Figure 6), the same direction pattern was still observed. The speed ranged 0-0.14, 0-0.11, 0-0.15, 0-0.12 m/s for high neap, low neap, high spring, and low spring tidal conditions respectively. In the bay mouth, the current flow is faster affecting the high turbulence rate. The maximum velocity was found in the eastern part within the bay.

According to the previous study Wisha *et al*. (2015) during 2nd transitional season 2014 in the

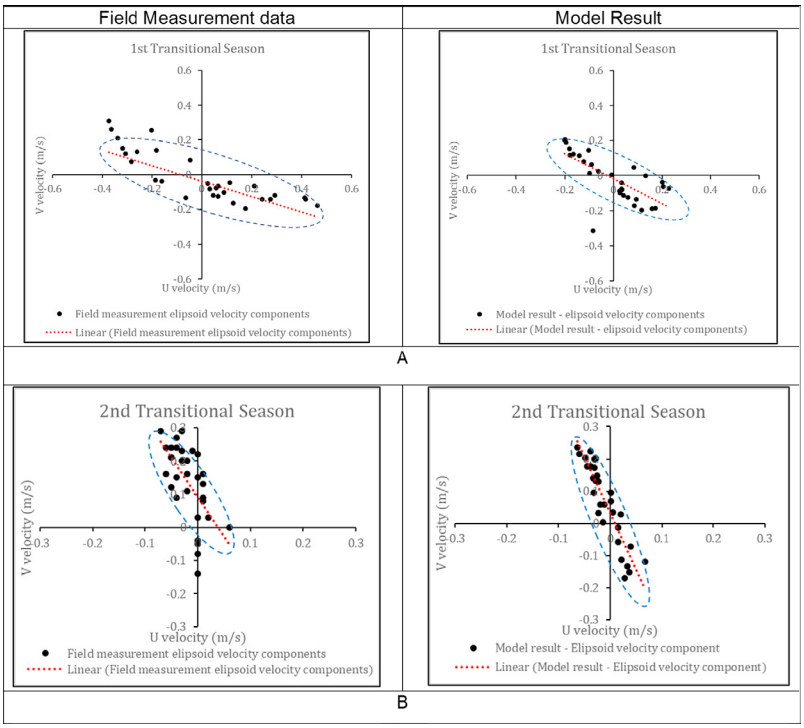

Figure 4. Model validation by using elliptical velocity component analysis on First Transitional (A) and Second Transitional Monsoon (B).

Banten Bay, the tidal current speed ranged 0-0.15 m/s for spring high tidal condition. In addition, the current direction is slightly different compared with the newer simulation, located in the west part within the bay where the speed is decline. That declination is caused by a rapid sediment deposition within the bay resulted by sand mining in the bay mouth triggering the unstable sediment transport in the surrounding (Rahmawan *et al*., 2017).

At neap low tidal condition, the current speed is slightly different, the attracting result is the direction predomination in the bay mouth that is totally different. It moves Northwestward in 2014 and toward North in

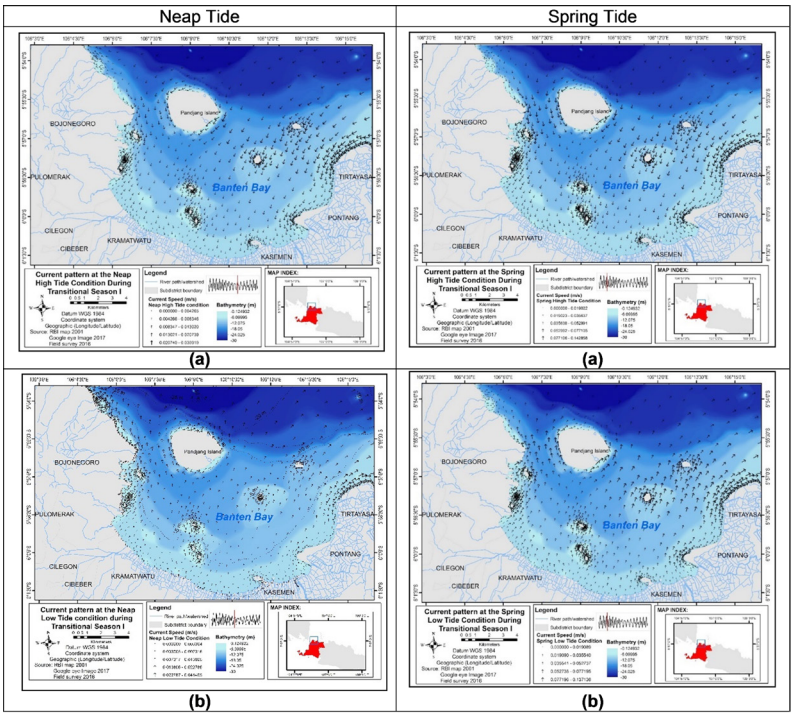

Figure 5. Tidal Current Simulation during Neap and Spring Tide in First Transitional Monsoon. (a) Flood Tide Phase (b) Ebb Tide Phase.

2015 simulation. At neap high tidal condition, there is no differentiation in current direction predomination between 2014 and 2015 simulation, but in the 2015 simulation result, the current speed is higher in the Pamujan Kecil Island ranged 0.06-0.13 m/s. At neap low tidal condition, the current direction is the same between 2014 and 2015 simulations, while, the current speed decreases approximately 0.06 m/s.

At neap tidal condition, the flow velocity is weaker than spring condition. It is because the gravity forces of the moon, the earth, and the sun become weak due to the upright astronomical position, so that the current generation is also weakened (Van Rijn, 2011; Lazure *et al*., 2009).

The long tidal wave from deeper ocean will release the energy into the shallow water and causes the coastal waters severely influenced by tidal conditions. The result of the model shows that the water moves into the open sea during low tidal condition, while, it flows perpendicularly to the land at the high tidal condition.

These circulations trigger turbulence, mixing, and water mass dynamic enhancement. According to Li & Zhong (2007) the tidal mixing in the bottom is stronger. It penetrates higher at high tidal than at low tidal condition causing a significant variation of material distribution over the high-low tidal cycle. There are insignificant changes in the residual circulation. At the spring tidal condition, the current velocity becomes higher due to the high astronomical forces triggering the higher elevation formed.

The strongest currents are observed in the east part within bay where the tidal flow is topographically controlled by the shallow sub tidal delta platform of the former Ciujung delta. Tidal currents inside the bay lag behind the tidal flow in the Java Sea, which generates horizontal velocity shears at the slope break north of the bay. Drift currents are in the order of 0.008 m/s and related to the local, monsoon-dominated wind climate (Hoekstra *et al*., 2002).

Consequently, regional differences in tidal currents and drift velocities contribute to the residual transport of sediment from the east to the central and southern part of the bay. In the past Dua Island, a bird sanctuary (Noor & Hasudungan, 2002) and former island, became attached to the mainland coast which has resulted in much more vulnerable conditions.

The characteristic of hydrodynamic in Banten Bay is also influenced by the seasonal wind-driven, resulting in different tidal current pattern in every level alteration. The current speed is also affected by the

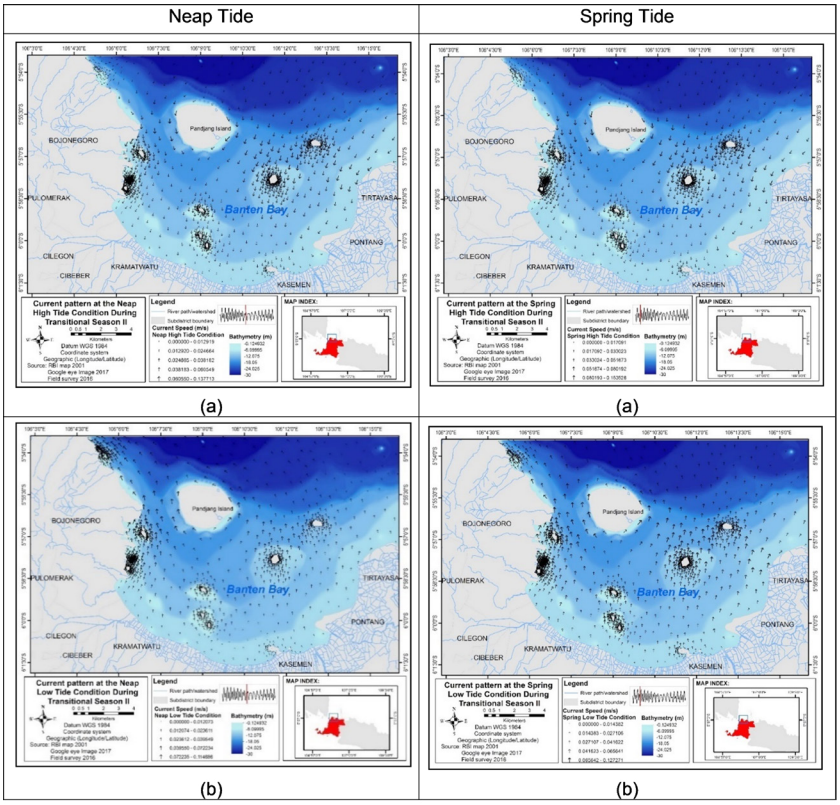

Figure 6. Tidal Current Simulation during Neap and Spring Tide in Second Transitional Monsoon. (a) Flood Tide Phase (b) Ebb Tide Phase.

tidal energy working in every single tidal change. It will lead the transport mechanism along the bay controlling the sediment transport in and out of the bay (Wisha & Heriati, 2016).

The hydrodynamics are influenced by the bathymetry profile. The average of water depth ranged from 0-30 meters (Shallow water) (Kulhandjian & Melodia, 2014). Bottom friction has a big role resisting the surface current flow. According to Ffield and Gordon (1996); Hendrawan & Ardana (2010), the bottom friction controls the magnitude of velocity components. It varies over the seabed depended on the bathymetry profile. When the elevation decreased (low tidal condition), the bottom friction enhanced, affecting the weak water mass dynamic. It triggers the accretion due to the minimal turbulence occurred.

Hydrodynamic condition has a significance role evoking the unstable abrasion and accretion along Banten Bay coast. According to Rahmawan et al. (2017) during 1991-2013, the abrasion reached 384.15 hectares and the accretion reached 425.50 hectares. The erosion is faster when the mining activity has been occurring (2003-2007). Resulting in unstable erosion and sedimentation within the bay.

CONCLUSION

The current direction patterned relatively the same for each tidal condition in both transitional seasons, slightly opposite in the neap low tidal condition between 1st and 2nd transitional season that moves toward Northwest and Northeast respectively. The current speed is higher in the spring tide phase than the neap tide phase ranged more/less 0-0.15 m/s during those two simulations where the strongest current flow was observed in the east part within the bay. Banten Bay is predominated by tidal current proved by the elliptical velocity component formed, slightly different in velocity and direction of rotary tidal current approximately 3-5 degrees differentiation between 1st and 2nd transitional season simulations. Hydrodynamic pattern differentiation of Banten Bay during two transitional monsoons has a role controlling transport mechanism in those two seasons, which induces the unstable sedimentation and erosion along Banten Bay coast.

ACKOWLEDGEMENTS

This research is a part of Sediment Quality Research Project which is funded by Research Center for Oceanography (RCO), Indonesian Institute of Sciences budget. We would like to show our gratitude to Dr. Dwi Hindarti as the coordinator who allowed the author to participate. As well as to Budi Wiryawan who supported the licensed software used to simulate hydrodynamic in this study.

REFFERENCE

Antony, C. & Unnikrishnan, A.S. (2013). Observed characteristics of tide-surge interaction along the east coast of India and the head of Bay of Bengal. Estuarine, Coastal and Shelf Science, 131, 6-11. Doi: 10.1016/j.ecss.2013.08.004.

Boon, J. D. (2013). Secrets of the tide: tide and tidal current analysis and predictions, storm surges and sea level trends. Elsevier.

Carter, G. S., & Merrifield, M. A. (2007). Open boundary conditions for regional tidal simulations. Ocean Modelling, 18(3-4), 194-209. Doi: 10.1016/j.ocemod.2007.04.003.

Douglas, R.M. (2001). Physical Oceanography. Dept of Geophysical Science. Univ of Chigago, Illinois.

Fang, G., Wang, Y., Wei, Z., Fang, Y., Qiao, F. & Hu, X. (2009). Interocean circulation and heat and freshwater budgets of the South China Sea based on a numerical model. Dynamics of Atmospheres and Oceans, 47(1), 55-72. Doi: 10.1016/j.dynatmoce.2008.09.003.

Fang, G., Susanto, R.D., Wirasantosa, S., Qiao, F., Supangat, A., Fan, B., Wei, Z., Sulistyo, B., and Li, S. (2010). Volume, Heat and Freshwater Transport from The South China Sea to Indonesian Seas in the Boreal Winter of 2007-2008. J. Geophys. Res, 115. C12020. Doi: 10.1029/2010JC006225.

Ffield, A. & Gordon, A.L. (1996). Tidal mixing signatures in the Indonesian Seas. Journal of Physical Oceanography, 26(9), 1924-1937. Doi: 10.1175/1520-0485(1996)026.

Garrett, C. & Kunze, E. (2007). Internal tide generation in the deep ocean. Annu. Rev. Fluid Mech., 39, 57-87. Doi: 10.1146/annurev.fluid.39.050905.110227.

Gordon, A.L., Susanto, R. D. & Vranes, K. (2003). Cool Indonesian Throughflow as A Consequence of Restricted Surface Layers Flow. Nature, 425, 824-828. Doi: 10.1038/nature02038.

Gordon, A.L., Sprintall, J., Van Aken, H.M., Susanto, D., Wijffels, S., Molcard, R., Ffield, A., Pranowo, W., & Wirasantosa, S. (2010). The Indonesian throughflow during 2004–2006 as observed by the INSTANT program. Dynamics of Atmospheres and Oceans, 50(2), 115-128. Doi: 10.1016/j.dynatmoce.2009.12.002.

Gordon, A.L., Huber, B.A., Metzger, E.J., Susanto, R.D., Hurlburt, H.E. & Adi, T.R. (2012). South China Sea throughflow impact on the Indonesian throughflow. Geophysical Research Letters, 39, L11602. Doi: 10.1029/2012L052021.

Hendrawan, I.G., & Ardana, I.K. (2010). Numerical calculation of phosphate transport in Benoa Bay, Bali. International Journal of Remote Sensing and Earth Sciences (IJReSES), 6(1). Doi: https://doi.org/10.1007/s13131-014-0434-5.

Hoekstra, P., Lindeboom, H., Bak, R., Bergh, G.V.D., Tiwi, D.A., Douven, W., Heun, J., Hobma, T., Hoitink, T., Kiswara, W., Meesters, E., Noor, Y., Sukmantalya, N., Nuraini, S. & Weering, T.V. (2002). Teluk Banten Research Programme: an integrated coastal zone management Study. Staple (Ed.) Scientific programme Indonesia - Netherlands Proceedings of a workshop held on February 12th, 2002. Bandung. Indonesia., pp: 59-70.

Holt, J.T., Allen, J.I., Proctor, R. & Gilbert, F. (2005). Error quantification of a high-resolution coupled hydrodynamic–ecosystem coastal–ocean model: part 1 model overview and assessment of the hydrodynamics. Journal of Marine Systems, 57(1), 167-188. Doi: 10.1016/j.jmarsys.2005.04.008.

King, M.A., Padman, L., Nicholls, K.W., Clarke, P.J., Gudmundsson, H., Kulessa, B. & Shepherd, A. (2011), Ocean tides in the Weddell Sea: new observations on the Filchner-Ronne and Larsen C ice shelves and model validation, J. Geophys. Res. (Oceans), 116(C06006), Doi: 10.1029/2011JC006949.

Kulhandjian, H. & Melodia, T. (2014). Modeling underwater acoustic channels in short-range shallow water environments. In Proceedings of the International Conference on Underwater Networks & Systems (p. 26). ACM.

Kvale, E.P. (2006). The origin of neap–spring tidal cycles. Marine Geology, 235(1), 5-18. Doi: 10.1016/j.margeo.2006.10.001.

Lazure, P., Garnier, V., Dumas, F., Herry, C. & Chifflet, M. (2009). Development of a hydrodynamic model of the Bay of Biscay. Validation of hydrology. Continental Shelf Research, 29(8), 985-997. Doi: 10.1016/j.csr.2008.12.017.

Li, M. & Zhong, L. (2009). Flood–ebb and spring–neap variations of mixing, stratification and circulation in Chesapeake Bay. Continental Shelf Research, 29(1), 4-14. Doi: 10.1016/j.csr.2007.06.012

Lukas, R., Yamagata, T. & McCreary, J.P. (1996). Pacific low-latitude western boundary currents and the Indonesian throughflow. Journal of Geophysical Research: Oceans, 101(C5), 12209-12216. Doi: 10.1029/96jc01204.

Mahardika, R.W., Ismanto, A. & Purwanto, P. (2015). Studi Perbandingan Simulasi Model Flow Model Fm Dan Adcirc Terhadap Pola Arus Pasut Perairan Teluk Lembar Lombok. Journal of Oceanography, 4(1), 206-214. [in bahasa].

Masoud, M., Babak, B. & vahid, C. (2012). Least Square Analysis of Noise-Free Tides Using Energy Conservation and Relative Concentration of Periods Criteria. Journal of the Persian Gulf (Marine Science), 3(8), 12-23.

Noor, Y.R. & Hasudungan, F. (2002). Observation of re-breeding of Black-headed Ibis (Threskiornis melanocephalus) in Pulau Dua, Serang, Journal of Indonesian Ornithological Society. (In Press)

Qu, T., Du, Y. & Sasaki, H. (2006). South China Sea throughflow: A heat and freshwater conveyor. Geophysical Research Letters, 33(23), L23617. Doi: 10.1029/2006gl028350.

Park, J., Heitsenrether, R., & Sweet, W.V. (2014). Water Level and Wave Height Estimates at NOAA Tide Stations from Acoustic and Microwave Sensors. NOAA Technical Report NOS CO-OPS 075. Silver Spring, Maryland, June 2014.

Poulain, P.M. (2013). Tidal currents in the Adriatic as measured by surface drifters. Journal of Geophysical Research: Oceans, 118(3), 1434-1444. Doi: 10.1002/jgrc.20147.

Rahmawan, G.A., Husrin, S. & Prihantono, J. (2017). Bathymetry Changes Analysis in Serang District Waters Caused by Seabed Sand Exploitation. Jurnal Ilmu dan Teknologi Kelautan Tropis, 9(1), 45-55. Doi: 10.28930/jitkt.v9i1.17916. [in Bahasa].

Siregar, S.N., Sari, L.P., Purba, N.P., Pranowo, W.S. & Syamsuddin, M.L. (2017). Pertukaran massa air di Laut Jawa terhadap periodisitas monsun dan Arlindo pada tahun 2015. DEPIK Jurnal Ilmu-Ilmu Perairan, Pesisir dan Perikanan, 6(1), 44-59. Doi: 10.13170/depik.6.1.5523. [In Bahasa].

Spaulding, M.L. & Mendelsohn, D.L. (1999). WQMAP: An integrated three-dimensional hydrodynamic and water quality model system for estuarine and coastal applications. Marine Technology Society Journal, 33(3), 38-54. Doi: 10.4031/mtsj.33.3.6.

Stewart, R.H. (2006). Introduction to Physical Oceanography. Dept of Oceanography. Texas A&M

Susanto, R.D., Ffield, A., Gordon, A.L. & Adi, T.R. (2012). Variability of Indonesian throughflow within Makassar Strait, 2004–2009. Journal of Geophysical Research: Oceans, 117(C9). C09013. Doi: 10.1029/2012jc008096.

Susanto, R.D., Wei, Z., Adi, R.T., Fan, B., Li, S. & Fang, G. (2013). Observations of the Karimata Strait througflow from December 2007 to November 2008. Acta Oceanologica Sinica, 32(5), 1-6. Doi: 10.1007/s13131-013-0307-3.

Tozuka, T., Qu, T., Masumoto, Y. & Yamagata, T. (2009). Impacts of the South China Sea Throughflow on seasonal and interannual variations of the Indonesian Throughflow. Dynamics of Atmospheres and Oceans, 47(1), 73-85. Doi: 10.1016/j.dynatmoce.2008.09.001.

Van Rijn, L.C. (2011). Analytical and numerical analysis of tides and salinities in estuaries; part I: tidal wave propagation in convergent estuaries. Ocean Dynamics, 61(11), 1719-1741. Doi: 10.1007/s10236-011-0453-0.

Wessel, P. & Smith, W.H. (1996). A global, self-consistent, hierarchical, high-resolution shoreline database. Journal of Geophysical Research: Solid Earth, 101(B4), 8741-8743. Doi: 10.1029/96jb00104.

Wicaksana, S., Sofian, I. & Pranowo, W. (2015). Karakteristik Gelombang Signifikan Di Selat Karimata Dan Laut Jawa Berdasarkan Rerata Angin 9 Tahunan (2005-2013). Omni-Akuatika, 11(2):33-40. Doi: 10.20884/1.oa.2015.11.2.37.

Wisha, U.J., Husrin, S. & Prihantono, J. (2015). Hydrodynamics Banten Bay During Transitional Seasons (August-September). Ilmu Kelautan, 20(2). 101-112. Doi: 10.14710/ik.ijms.20.2.101-112. [in Bahasa].

Wisha, U.J., & Heriati, A. (2016). Bathymetry and Hydrodynamics in Pare Bay Waters During Transitional Seasons (September-October). Omni-Akuatika, 12(2). 1-10. Doi: 10.20884/1.oa.2016.12.2.98.

Wisha, U.J., Al Tanto, T., Pranowo, W. S. & Husrin, S. (2017). Current movement in Benoa Bay water, Bali, Indonesia: Pattern of tidal current changes simulated for the condition before, during, and after reclamation. Regional Studies in Marine Science. 18, 177-187. Doi: 10.1016/j.rsma.2017.10.006.

Zhao, D.H., Shen, H.W., Tabios III, G.Q., Lai, J.S. & Tan, W.Y. (1994). Finite-volume two-dimensional unsteady-flow model for river basins. Journal of Hydraulic Engineering, 120(7), 863-883. Doi: 10.1061/(asce)0733-9429(1994)120:7(863).